Version of Record: https://www.sciencedirect.com/science/article/pii/S0040603119306422
Manuscript_3a1a7464344b37c60f890d5a13d769f5

Kinetic modeling using temperature as an on-line measurement: Application to the hydrolysis of acetic anhydride, a revisited kinetic model.

Elizabeth Antonia Garcia-Hernandez[1], *Camilla Ribeiro Souza*[1], *Lamiae Vernières-Hassimi*[1], *Sébastien Leveneur**[1,2]

[1]*Normandie Univ, INSA Rouen, UNIROUEN, LSPC, EA4704, 76000 Rouen, France, E-mail: sebastien.leveneur@insa-rouen.fr*

[2]*Laboratory of Industrial Chemistry and Reaction Engineering, Johan Gadolin Process Chemistry Centre, Åbo Akademi University, Biskopsgatan 8, FI-20500 Åbo/Turku, Finland.*

Abstract. The use of calorimeter in chemical reaction engineering is a powerful tool to estimate kinetic constants. Indeed, reaction temperature is used as an online analytical signal. Nevertheless, the thermal characterization of the calorimeter must be done to avoid wrong estimation. The hydrolysis of acetic anhydride was used as a reaction model in a handmade calorimeter, because it is a fast and exothermic reaction. Several research groups have studied this reaction without taking into account the autocatalytic effect due to the production of acetic acid. To fill this gap, a kinetic model was developed by taking this phenomenon and in a thermally characterized handmade calorimeter. The estimated kinetic constants in the handmade calorimeter were found to be similar than in the established calorimeter Mettler Toledo RC1.

KEYWORDS: calorimeter, exothermic reaction, isoperibolic mode, kinetic modeling.

© 2019 published by Elsevier. This manuscript is made available under the CC BY NC user license
https://creativecommons.org/licenses/by-nc/4.0/

HIGHLIGHTS

- Thermal characterization of a calorimeter
- Kinetic model using reaction temperature as online observable
- Kinetic model for acetic anhydride hydrolysis taking into account autocatalytic effect

1.INTRODUCTION

Calorimetry is a science that finds its roots with the works of Joseph Black, Antoine Lavoisier and Pierre-Simon Laplace. It is an important thermal analytical tool in different fields such as material science, polymer, chemistry or chemical engineering. One can get fundamental thermal and thermodynamic data of different compounds by using different thermal modes.

In chemical engineering, calorimetry allows to measure/estimate specific heat capacities of chemicals [1–4] and reaction enthalpies [5–7] . It is also the appropriate tool in process safety and more particularly in thermal risk assessment to determine risk parameters such as time-to-maximum-rate under adiabatic conditions TMR_{ad} or adiabatic temperature rise ΔT_{ad}. The knowledge of these safety parameters allow to evaluate the thermal risk of a chemical process [7–12] .

Another benefit of calorimeter is in chemical reaction engineering, where reaction temperature is used as an online measurement signal. The use of calorimeter to estimate rate constants has significantly increased these last years, essentially for fast and exothermic reactions.

The use of reaction temperature or heat-flow rate released as online signals to evaluate the kinetics of a reaction was used by several research groups [13–19] . The development of calorimeters has participated to the development of this approach. Nevertheless, one should also take into account different thermal phenomena such as specific heat capacity of the inserts or heat loss [16] .

Hydrolysis of acetic anhydride is frequently used as a calibration reaction for calorimeters [13,20]. This reaction was studied by several research groups:

-Wiseman [21] used pH as an online analytical method but he did not include the energy balance,

-Susanne et al. [22] used NMR as an online method but they did not include energy balance,

-Hirota et al.[23] have used the temperature to make the kinetic estimation without taking into account the autocatalytic effect of the reaction,

-Zogg et al. [24,25] studied this reaction by combining calorimetric and IR techniques, but they assumed a first order reaction,

-Gomez Garcia et al. [26] used this reaction as an example for thermal stability,

-Asiedu et al. [27] studied this reaction under adiabatic mode but with a first order approach.

This reaction is known to be autocatalytic due to the dissociation of the product acetic acid. Nevertheless, none of these research groups have developed a kinetic model taking into account this phenomenon for this reaction.

The objective of this article is to develop a kinetic model including the autocatalytic effect and the different thermal phenomena. To estimate the kinetic constants, experiments under isoperibolic mode was performed in a hand-made calorimeter. The thermal properties of this calorimeter were investigated. To validate the developed kinetic model in the hand-made calorimeter, a comparison with the RC1 Mettler-Toledo calorimeter was done.

2.EXPERIMENTAL SECTION

2.1. Materials

The following chemicals were used: ACS reagent acetic anhydride (purity ⩾99%) and distilled water.

2.2. Experimental Setup

Kinetic experiments for the hydrolysis of acetic anhydride were carried out in the hand-made calorimeter composed of a 300 mL jacketed glass reactor equipped with accurate temperature probes, a calibration probe to measure the global heat transfer coefficient, a mechanical stirrer and reflux condenser. The internal diameter of the jacketed reactor was 10 cm, and the mechanical stirrer was a pitched blade turbine impeller (diameter 3.8 cm and 4 blades). The inlet temperature of condenser was fixed at 10°C to avoid the loss of liquid phase compounds. Experiments were performed under isoperibolic and semi-batch mode. Fig. 1 shows a simplified scheme of the reactor setup.

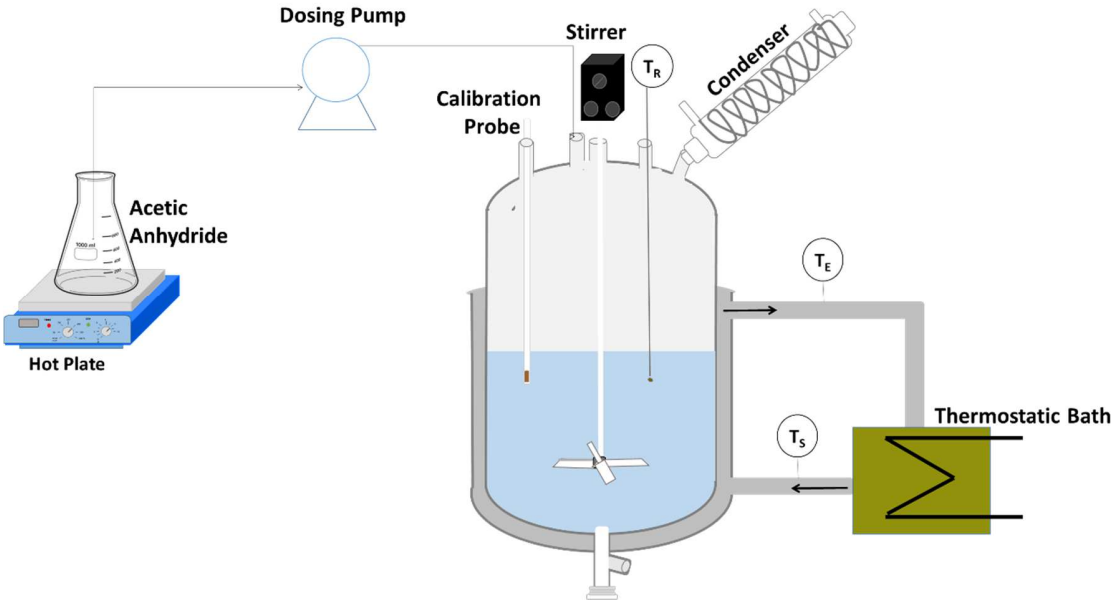


Fig. 1. Schematic representation of the experimental setup.

2.3 Thermal characterization of the calorimeter

The goals of these experiments are to measure the heat transfer coefficient between the reaction mixture and heat carrier, evaluate the heat loss and measure the specific heat capacities of the inserts.

- Measurement of heat transfer coefficient

To determine the heat transfer coefficient, an electrical calibration was used. For that, the reactor was filled with a solution and heated to the desired temperature in the absence of reaction and under isoperibolic conditions. When the solution temperature was stable, a known electrical power (Joule heating) was provided for around 10 minutes and then switched off. The evolution of the solution temperature was recorded. One can find a detailed description of this method in previous article of our group [28,29].

- Measurement of specific heat capacity of the inserts.

The procedure described in reference [30] was used. The thermostatic bath was set to a temperature but the heat carrier did not circulate in the reactor jacket. At the same time the reactor was filled with water at room temperature. When the thermostatic bath reached the desired temperature, the pump system was switched on to allow the circulation of the heat carrier in the jacket. Both temperature, jacket and water temperature were recorded. These measurements were carrying out at three different temperatures (40, 60 and 80 °C).

- Evaluation of heat loss

The thermostatic bath was set at a temperature and the circulation of the heat carrier was switched on. The reactor was filled with water and heated to the desired temperature. When the water temperature was at the same temperature as the jacket one, the circulation of the heat carrier stopped (defined as time zero) and removed from the jacket. The water temperature was recorded. The experiments were carrying out at three different temperatures (40, 60 and 80 °C).

2.4 Kinetic experiments in calorimeter

Kinetic experiments were performed in semi-batch mode where acetic anhydride was added into the reactor. Table 1 shows the experimental matrix.

Table 1
Experimental matrix in handmade calorimeter with an agitation speed of 400 rpm.

RUN	Added volume of acetic anhydride (L)	Time of addition (s)	Acetic anhydride volumetric flow rate (L s^{-1})	Initial volume of water (L)	Initial jacket and reaction temperature (°C)	Feed temperature (°C)
1	0.09	7.00	0.0128	0.19	30.07	27.00
2	0.09	7.00	0.0128	0.19	39.73	28.00
3	0.09	7.00	0.0128	0.19	49.34	48.00
4	0.09	7.00	0.0128	0.19	59.17	58.00
5	0.13	600.00	0.0002	0.14	49.58	23.00

2.5 Kinetic experiment in Mettler Toledo calorimeter RC1

The Mettler™ RC1 is a jacketed-glass reactor calorimeter of 2 L presented in Fig. 2. It is equipped with a Pt100 temperature probe, an electrical calibration heating and a feed system (a dosing pump and a balance, with measurement of the feed temperature). The heating–cooling system works within a temperature range of −15 to +200°C. WinRCNT software solves the energetic balance on the reaction mass.

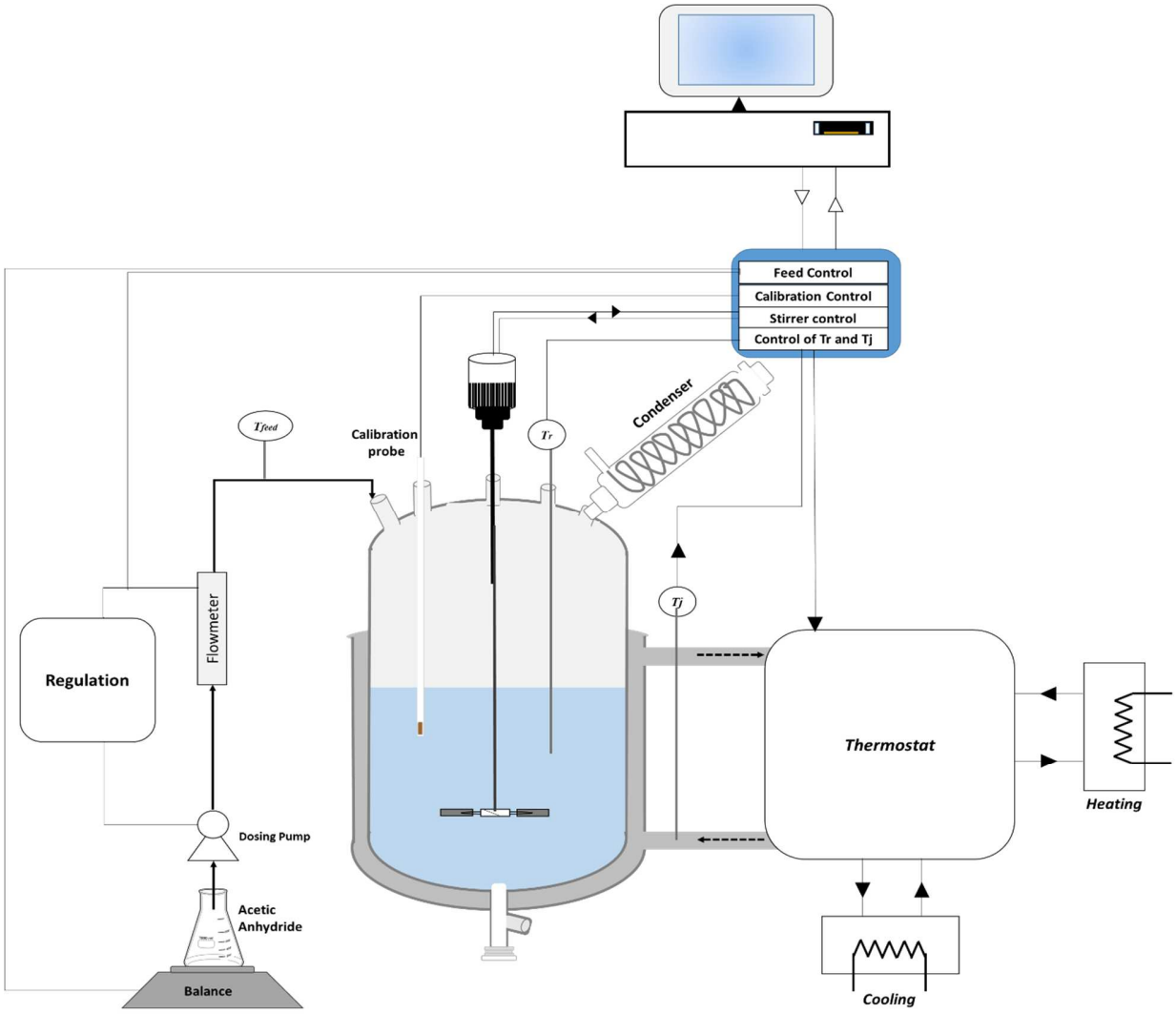


Fig. 2. Schematic representation of the reaction calorimeter RC1.

Table 2

Experimental matrix for acetic anhydride hydrolysis in RC1 calorimeter with an agitation speed of 400 rpm.

RUN	Added volume of acetic anhydride (L)	Time of addition (s)	Acetic anhydride volumetric flow rate (Ls^{-1})	Initial volume of water (L)	Initial jacket and reaction temperature (°C)	Feed temperature (°C)
6	0.2295	300	0.0007	1.2000	39.88	22.86
7	0.464	300	0.0015	0.9658	39.87	22.20

3. RESULTS AND DISCUSSION

3.1 Kinetics

To take into account the autocatalysis effect of acetic anhydride hydrolysis, the reaction can be divided in two routes: catalyzed and non-catalyzed one. Fig. 3 shows the non-catalyzed reaction mechanism.

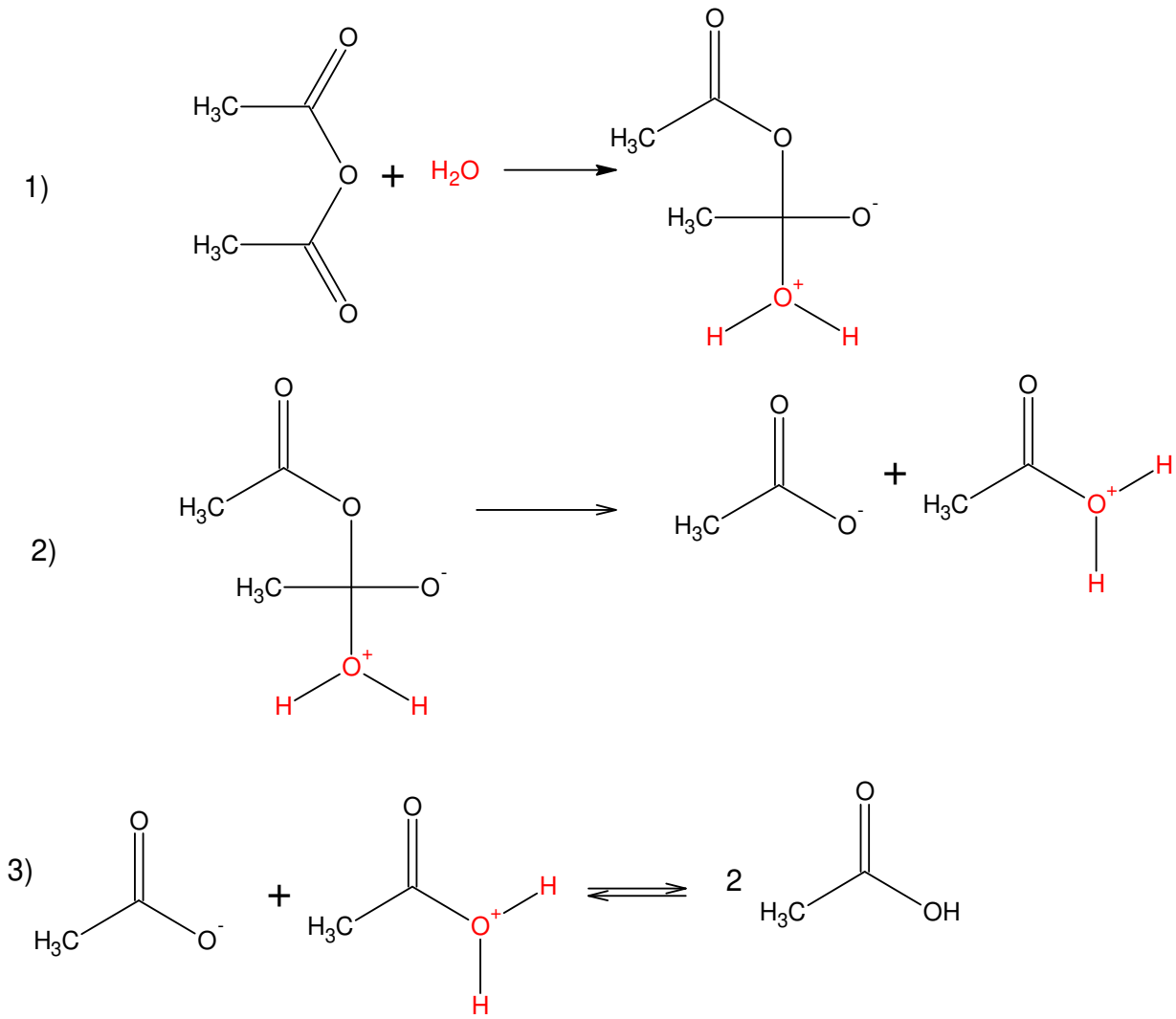
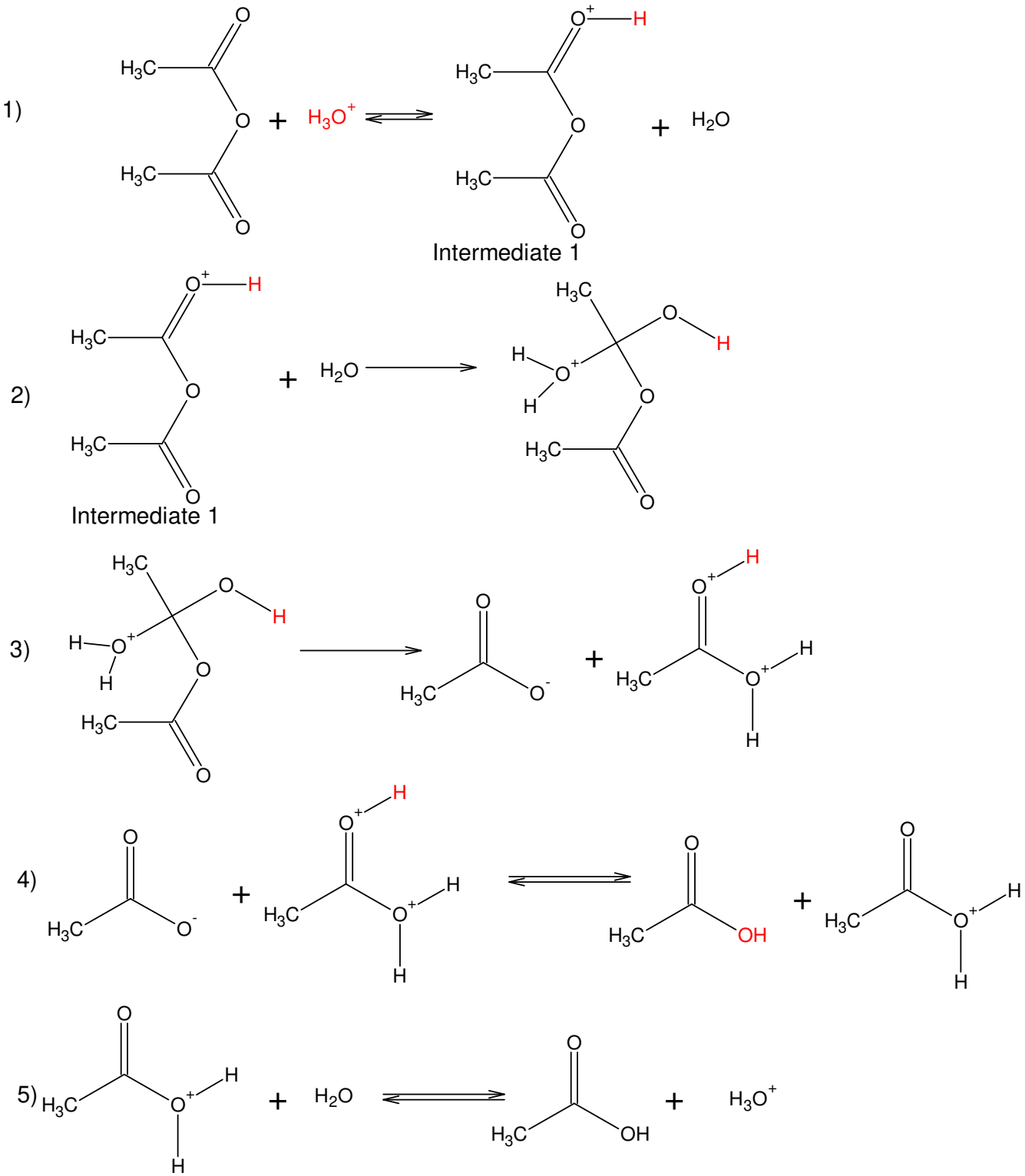


Fig. 3. Non-catalyzed reaction mechanism.

From Fig. 3, the rate-determining step can be assumed to be step 1. Thus, the non-catalyzed hydrolysis rate can be expressed as:

$$R_{Hydrolysis-non.cat} = k_{Hydrolysis-non.cat} \times [Anhydride\ Acetic] \times [H_2O] \quad (1)$$

Fig. 4 shows the reaction mechanism by the catalyzed route.



146
147 Fig. 4. Catalyzed reaction mechanism.

148 Reaction 2 (Fig. 4) is assumed to be the rate determining step, thus the rate of catalyzed
149 hydrolysis can be expressed as

150 $$R_{Hydrolysis-cat} = k_{Hydrolysis-cat} \times [Intermediate_1] \times [H_2O] \quad (2)$$

151 Steady-state approximation is applied on reaction 1 (Fig. 4), thus one gets

152 $$K_1 = \frac{[Intermediate_1] \times [H_2O]}{[Acetic\ anhydride] \times [H_3O^+]} \quad (3)$$

153 By combining Eqs (2) and (3), one gets:

154 $$R_{Hydrolysis-cat} = k_{Hydrolysis-cat} \times K_1 \times \frac{[Acetic\ anhydride] \times [H_3O^+]}{[H_2O]} \times [H_2O] \quad (4)$$

155 Hence, by adding Eqs (1) and (4), the rate of hydrolysis becomes

156 $$R_{Hydrolysis} = R_{Hydrolysis-non.cat} + R_{Hydrolysis-cat}$$

157 $$= ([Acetic\ anhydride] \times [H_2O]) \times \left[k_{Hydrolysis-non.cat} + k_{Hydrolysis-cat} \times K_1 \times \frac{[H_3O^+]}{[H_2O]}\right] \quad (5)$$

158 By noting $k'_{Hydrolysis-cat} = k_{Hydrolysis-cat} \times K_1$, then eq (5) becomes

159 $$R_{Hydrolysis} = ([Acetic\ anhydride] \times [H_2O]) \times \left[k_{Hydrolysis-non.cat} + k'_{Hydrolysis-cat} \frac{[H_3O^+]}{[H_2O]}\right]$$

160 (6)

161 Both rate constants were estimated in this study.

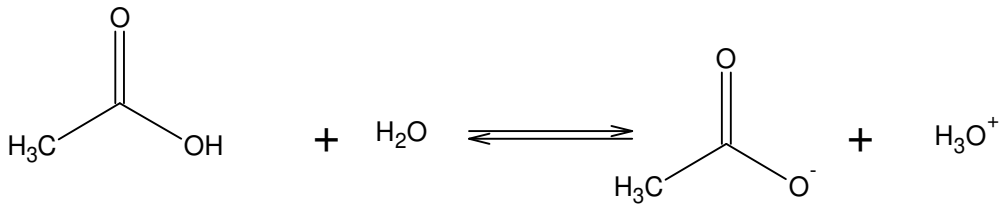
162

163

164

165 3.2 Sources of hydroxonium ion

166 The autoprotolysis of water was neglected in this study. The source of hydroxonium ion was
167 mainly due to the dissociation of the product acetic acid as illustrated by Scheme 1.



168

169 Scheme 1. Dissociation of acetic acid.

170

171 Mass balance of the organic species gives

172 $$[Acetic\ anhydride]_{FEED} = [Acetic\ anhydride] + \frac{1}{2}.[Acetic\ acid] + \frac{1}{2}.[CH_3COO^-] \quad (7)$$

173 The dissociation of acetic acid is fast, thus the dissociation constant, $K^C_{Acetic\ acid}$, can be
174 expressed as

175 $$K^C_{Acetic\ acid} = \frac{[\mathrm{CH_3COO^-}]\times[\mathrm{H_3O^+}]}{[\mathrm{CH_3COOH}]\times[\mathrm{H_2O}]} = \frac{K^T_{Acetic\ acid}}{55.56} \quad (8)$$

176 $K^T_{Acetic\ acid}$ is the true thermodynamic constant expressed according to Sue et al. [31].

177 According to the electroneutrality principle, the concentration of cation and anion species are
178 the same.

179 $$[H_3O^+] \approx [CH_3COO^-] \quad (9)$$

180 By combining Eqs (8) and (9), the acetic acid concentration can be expressed as

181 $$[\mathrm{CH_3COOH}] = \frac{[\mathrm{H_3O^+}]^2}{K^C_{Acetic\ acid}\times[\mathrm{H_2O}]} \quad (10)$$

Eqs (10) and (9) are introduced in Eq (7) leading to

$$[Acetic\ anhydride]_{FEED} = [Acetic\ anhydride] + \frac{1}{2}.\frac{[H_3O^+]^2}{K^C_{Acetic\ acid} \times [H_2O]} + \frac{1}{2}.[H_3O^+]$$

equivalent to

$$\frac{1}{2}.\frac{[H_3O^+]^2}{K^C_{Acetic\ acid} \times [H_2O]} + \frac{1}{2}.[H_3O^+] + [Acetic\ anhydride] - [Acetic\ anhydride]_{FEED} = 0 \quad (11)$$

By taking into account only the positive roots of Eq (11), one gets

$$[H_3O^+] = K^C_{Acetic\ acid}.[H_2O].\left[-\frac{1}{2} + \sqrt{\frac{1}{4} - \frac{2}{K^C_{Acetic\ acid} \times [H_2O]}.([Acetic\ anhydride] - [Acetic\ anhydride]_{FEED})}\right] \quad (12)$$

3.3 Mass balances

As mentioned in the experimental section, experiments were performed in semi-batch mode with the addition of acetic anhydride in the reactor.

Mass balances for acetic anhydride, acetic acid and water lead to the following ordinary differential equations:

$$\frac{d[Acetic\ anhydride]}{dt} = \frac{Q}{V_R} \times ([Acetic\ anhydride]_{FEED} - [Acetic\ anhydride]) - R_{Hydrolysis} \quad (13)$$

$$\frac{d[Water]}{dt} = -[Water] \times \frac{Q}{V_R} - R_{Hydrolysis} \quad (14)$$

$$\frac{d[Acetic\ acid]}{dt} = -[Acetic\ acid] \times \frac{Q}{V_R} + 2 \times R_{Hydrolysis} \quad (15)$$

$$\frac{dV_R}{dt} = Q \quad (16)$$

where, Q is the volumetric flow rate, $[Acetic\ anhydride]_{FEED}$ is the concentration of acetic anhydride in the feed.

3.4 Energy balance

For a semi-batch reactor under isoperibolic conditions, energy balance on the reaction mixture phase can be expressed as [28,32]:

$$q_{acc} = q_{reaction} + q_{exchange\ with\ heat\ carrier} + q_{loss} + q_{dosing} + q_{solvation}$$

$$\Leftrightarrow \left(m_R.\widehat{C_{P_R}} + m_{ins}.\widehat{C_{P_{ins}}}\right) \times \frac{dT_R}{dt} = -R_{Hydrolysis} \times V_R \times \Delta H_{R,Hydrolysis} + U \times A \times \left(T_j - T_R\right) + UA_{loss} \times (T_{ambient} - T_R) + Q \times \overline{C_{P_{Acetic\ Anhydride}}} \times [Acetic\ anhydride]_{FEED} \times (T_{FEED} - T_R) - \frac{\Delta H_{solvation} \times Q}{V_{molar}\ x\ (Acetic\ Anhydride)}$$

(17)

Heat capacities of the different species at stake were estimated by using Aspen Plus and the UNIQUAC thermodynamic model. Each term of Eq (17) is explained below.

*Accumulated heat-flow rate $q_{acc} = \left(m_R.\widehat{C_{P_R}} + m_{ins}.\widehat{C_{P_{ins}}}\right) \times \frac{dT_R}{dt}$

The specific heat capacity of the reaction mixture $\hat{C}_{P_R}$(J.kg^{-1}.K^{-1}) can be expressed as

$$\hat{C}_{P_R} = \omega_W \times \hat{C}_{P_W} + \omega_{Acetic\ anhydride} \times \hat{C}_{P_{Acetic\ anhydride}} + \omega_{Acetic\ acid} \times \hat{C}_{P_{Acetic\ acid}}$$

(18)

The specific heat capacity of a compound with temperature can be expressed as

$$\frac{\hat{C}_{P_i}(T)}{\hat{C}_{P_i}(T_{Ref})} = A.T^2 + B.T + C \qquad (19)$$

Fig. 5 shows the evolution of $\frac{\hat{C}_{P_i}(T)}{\hat{C}_{P_i}(T_{Ref=313.15K})}$ for water, acetic anhydride and acetic acid based on AspenPlus database.

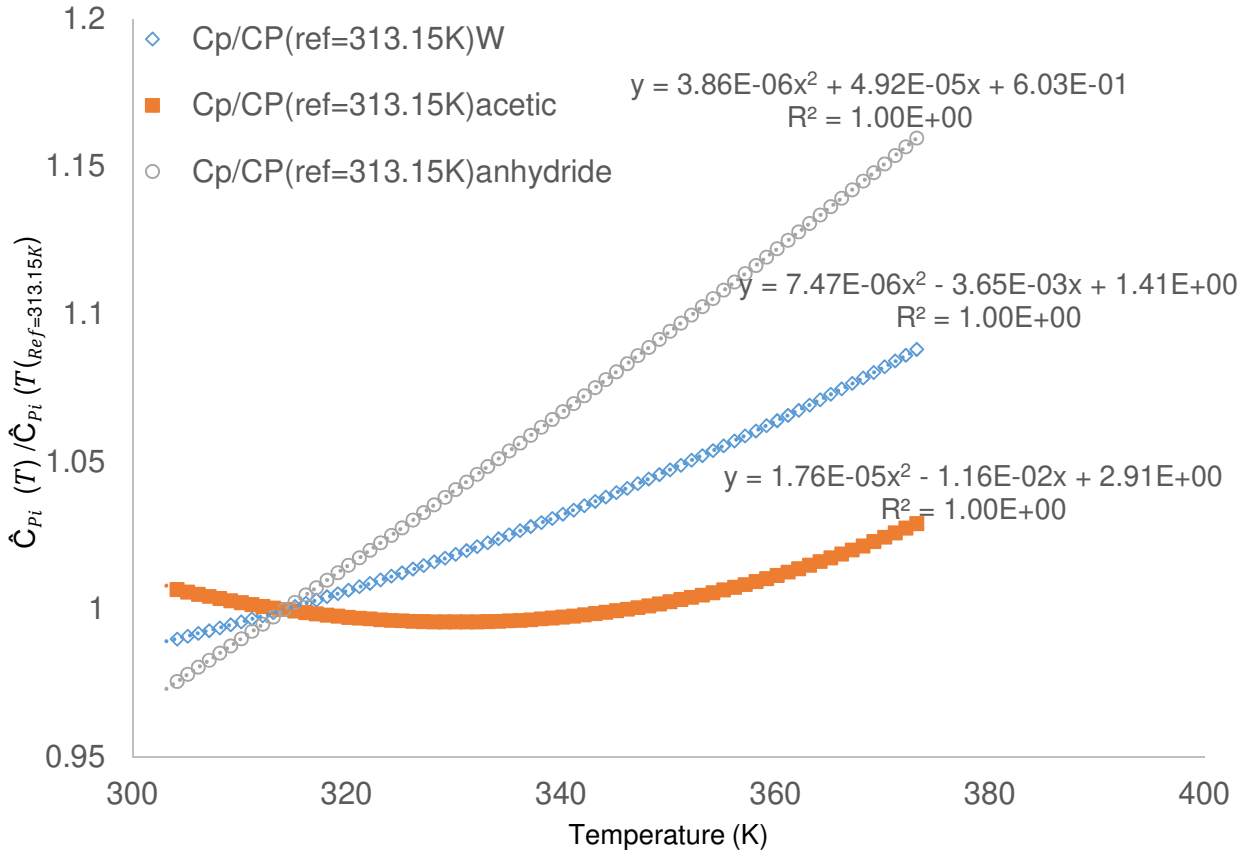


Fig. 5. $\frac{\hat{C}_{P_i}(T)}{\hat{C}_{P_i}(T_{Ref=313.15K})}$ versus temperature T/K.

Table 3
Specific heat capacity parameters.

	Water	Acetic acid	Acetic anhydride
Cp(313.15K)	4.18008	1.33385	1.63724
A	7.47E-06	$1.76 \cdot 10^{-05}$	$3.86 \cdot 10^{-06}$
B	-0.0036	-0.0116	$5.00 \cdot 10^{-05}$
C	1.4081	2.911	0.6032

The evaluation of the term $m_{ins}.\widehat{C_{P_{ins}}}$ is detailed in chapter 3.5. Reactor characteristic.

*Heat-flow rate due to chemical reaction $q_{reaction} = -R_{Hydrolysis} \times V_R \times \Delta H_{R,Hydrolysis}$

From Zogg et al. [24] , the enthalpy of hydrolysis, $\Delta H_{R,Hydrolysis}$, can be estimated to be equal to -60 kJ/mol. The term $V_R$stands for the reaction volume.

*Heat-flow rate exchange with heat carrier $q_{exchange\ with\ heat\ carrier} = U \times A \times (T_j - T_R)$

In chapter 3.5, the determination of U and A is explained. The terms T_j and T_R are the jacket and reaction temperatures, respectively.

*Heat flow rate loss $q_{loss} = UA_{loss} \times (T_{ambient} - T_R)$

The estimation of this loss is explained in chapter 3.5.

*Heat flow rate due to dosing $q_{dosing} = Q \times \overline{C_{P_{Acetic\ Anhydride}}} \times [Acetic\ anhydride]_{FEED}\ x\ (T_{FEED} - T_R)$

where, $\overline{C_{P_{Acetic\ Anhydride}}}\ (J\ mol^{-1}\ K^{-1})$ is the molar heat capacity of acetic anhydride. The concentration of acetic anhydride in the feed is $[Acetic\ anhydride]_{FEED} = 10.58\ mol.L^{-1}$. The term Q is the feeding volumetric flow-rate.

*Heat flow rate of solvation $q_{solvation} = -\frac{\Delta H_{solvation} \times Q}{V_{molar}\ x\ (Acetic\ Anhydride)}$

From Zogg et al. [24], the heat of solvation of acetic anhydride $\Delta H_{solvation}$is equal to + 3000 J/mol when the reaction temperature is higher than 40°C. The molar volume of acetic anhydride is equal to 0.0944 L mol^{-1} [33].

255 3.5 Reactor characteristic

256 The relationship between the reaction volume and the surface A was found to be

257 $$\mathrm{A}(m^2) = 0.0817 \times V(L) \quad (21)$$

258 To evaluate the heat transfer coefficient U during the reaction, one can use the sum of thermal
259 resistances using the thin wall approximation [34-35] .

260 $$\frac{1}{U} = \frac{1}{h_R} + \frac{d_{Wall}}{\lambda_{Wall}} + \frac{1}{h_j} \quad (22)$$

261 where, $\frac{1}{h_R}$ and $\frac{1}{h_j}$ represent the convective resistance to the heat transfer from the reaction side
262 and jacket side, respectively; d_w is the thickness of the glass wall between reaction mixture and
263 the heat carrier fluid, and λ_{Wall} is the heat conductivity of the glass wall.

264 The term $\frac{1}{h_R}$can change during the reaction, and the term $\frac{d_{Wall}}{\lambda_{Wall}} + \frac{1}{h_j}$ can be merged to a
265 constant and noted by $\frac{1}{\varphi_R}$. Eq. (22) becomes now:

266 $$\frac{1}{U} = \frac{1}{h_R} + \frac{1}{\varphi_R} \quad (23)$$

267 Under isothermal conditions and in the absence of chemical reactions, the properties of the
268 fluid and geometrical factors are constant. Thus the internal heat transfer coefficient can be
269 expressed as

270 $$\frac{1}{h_R} = Const \times \left(\frac{\mu_R}{\rho_R^2 \times \hat{C}_{P_R} \times \lambda_R^2}\right)^{1/3} \times \left(\frac{d_R^3}{d_s^2}\right)^{1/3} \times \left(\frac{1}{N^2}\right)^{1/3} \quad (24)$$

271 where,

Const is a constant,

μ_R is the dynamic viscosity of the reaction mixture in kg m^{-1} s^{-1},

ρ_R is the density of the reaction mixture in kg m^{-3},

$\hat{C}_{P_R}$ is the specific heat capacity of the reaction mixture in J kg^{-1} K^{-1},

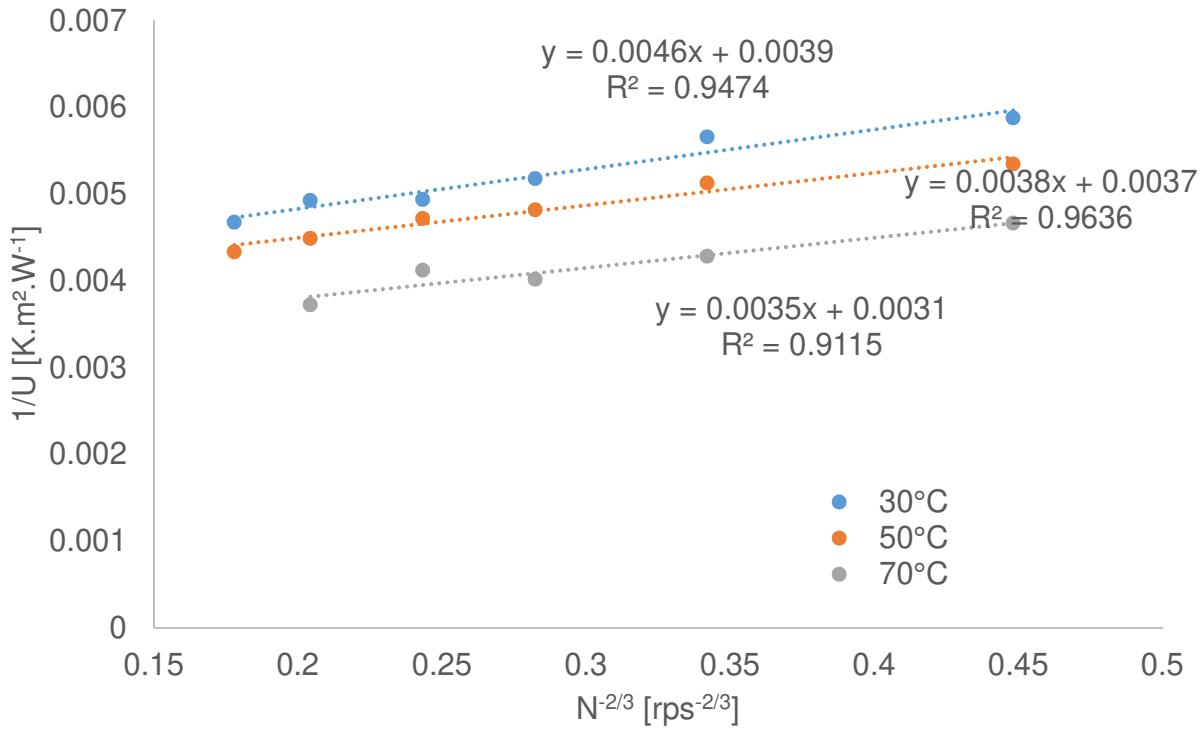
λ_R is the thermal conductivity of the reaction mixture in W m^{-1} K^{-1},

d_R is the reactor diameter in m,

N is the rotating speed in round per second,

d_s is the stirrer diameter in m.

Fig. 6 shows the evolution of $\frac{1}{U}$ versus $\left(\frac{1}{N^2}\right)^{1/3}$, also known as Wilson plot. To evaluate the values of $\frac{1}{\varphi_R}$ and $\frac{1}{h_R}$, a mixture containing 56 wt% of acetic acid was used as a representative one.



283

284 Fig. 6. Wilson plot 1/U versus $N^{-2/3}$ with a weight percentage of acetic acid of 56 %.

285

286 From Fig. 6, the values of $\frac{1}{\varphi_R}$ and $\frac{1}{h_R}$ can be assumed temperature independent. The values of

287 $\frac{1}{\varphi_R}$ is evaluated to 0.0035 K m^2 W^{-1} and $\frac{1}{h_R}$ to 0.0011 K m^2 W^{-1} at 400 rpm.

288

289 *Determination of specific heat capacity of inserts

290 In the absence of chemical reactions, the energy balance can be expressed as

291 $$\left(\mathrm{m}_R.\widehat{C_{P_R}} + \mathrm{m}_{ins}.\widehat{C_{P_{ins}}}\right) \times \frac{dT_R}{dt} = U \times A \times \left(T_j - T_R\right) \quad (26)$$

292 By assuming that specific heat capacity is constant on small temperature range, thus Eq. (26)

293 can be integrated as

294 $$\ln \frac{T_R - T_j}{T_{R0} - T_{j0}} = \frac{-U \times A}{\left(\mathrm{m}_R.\widehat{C_{P_R}} + \mathrm{m}_{ins}.\widehat{C_{P_{ins}}}\right)} \times t \quad (27)$$

295 The term $\mathrm{m}_{ins}.\widehat{C_{P_{ins}}}$ was equal to 29.95 J K^{-1}.

296 *Determination of the heat loss q_{loss}

297 Heat losses may then occur on the top side and on lateral or jacket side. Assuming a same heat

298 loss coefficient on both sides, since heat losses are limited by external natural convection on

299 both areas, the energy balance can then be described by

300 $$\left(\mathrm{m}_R.\widehat{C_{P_R}} + \mathrm{m}_{ins}.\widehat{C_{P_{ins}}}\right) \times \frac{dT_R}{dt} = UA_{loss} \times (T_{ambient} - T_R) \quad (28)$$

301 By assuming that heat capacity and UA_{loss} is temperature independent, thus Eq. (28) becomes

302 $$\ln \frac{T_R - T_{ambiant}}{T_{R0} - T_{ambiant0}} = \frac{-UA_{loss}}{\left(\mathrm{m}_R.\widehat{C_{P_R}} + \mathrm{m}_{ins}.\widehat{C_{P_{ins}}}\right)} \times t \quad (29)$$

303 We have found that UA_{loss} is equal to 0.053 W K^{-1}.

304

305 3.6 Modeling stage.

306 The system of ordinary differential Eqs (13)-(17) were solved out by the ODESSA solver.
307 Reaction temperature was used as an observable.

308 Simplex ad Levenberg-Marquardt algorithms were used to estimate the kinetic constants
309 $(k'_{Hydrolysis-cat}(T_{ref});\ Ea_{Hydrolysis-cat};\ k_{Hydrolysis-non.cat}(T_{ref})\ and\ Ea_{Hydrolysis-non.cat}$.

310 The rate constants at a temperature T were estimated by using a modified Arrhenius equation:

311 $$k'_{Hydrolysis-cat}(T) = k'_{Hydrolysis-cat}(T_{ref}) \times exp\left(\frac{-Ea_{Hydrolysis-cat}}{R} \times \left(\frac{1}{T} - \frac{1}{T_{ref}}\right)\right) \quad (30)$$

312 $$k_{Hydrolysis-non.cat}(T) = k_{Hydrolysis-non.cat}(T_{ref}) \times exp\left(\frac{-Ea_{Hydrolysis-non.cat}}{R} \times \left(\frac{1}{T} - \frac{1}{T_{ref}}\right)\right)$$

313 (31)

314 The solver and algorithms were implemented in the software ModEst [36]. The optimization
315 algorithms minimized the following objective function ω

316 $$\omega = \left(y_{exp} - y_{model}\right)^2 \quad (32)$$

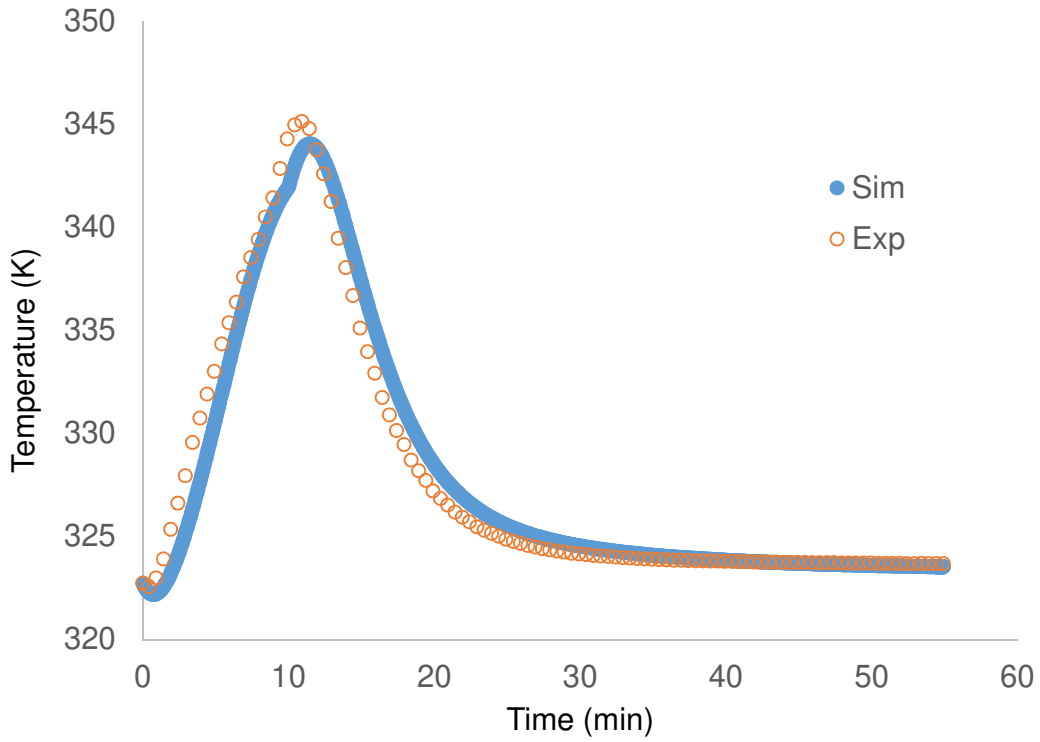
317 The coefficient of determination was expressed as

318 $$R^2 = 1 - \frac{(y_i - \hat{y}_i)^2}{(y_i - \bar{y})^2} \quad (33)$$

319

320

321 Figs. 7-8 show the fitting of the model to the experimental data for Runs 5 and 4. One can
322 notice that the model fits the experimental data. The value of the coefficient of determination
323 was found to be 99.15%. The reliability of the developed model is confirmed by the parity plot
324 (Fig. 9).



325

326 Fig. 7. Fitting of the model to the experimental data for Run 5.

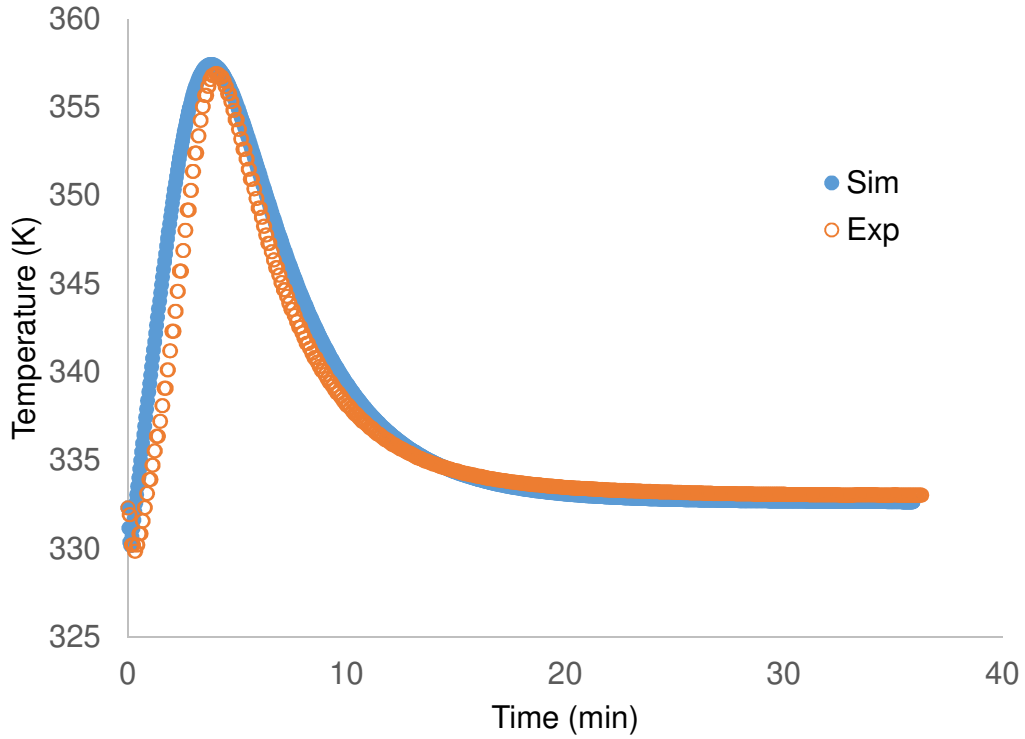
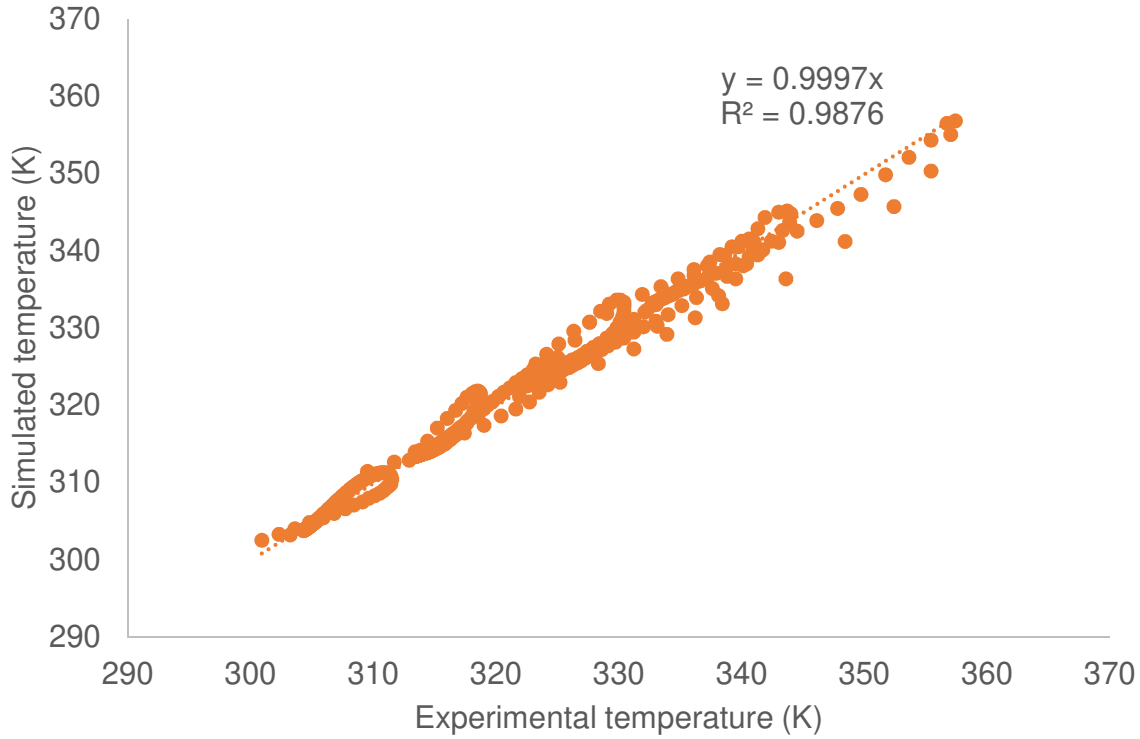


Fig. 8. Fitting of the model to the experimental data for Run 4.



330

331 Fig. 9. Parity plot.

332

333 Table 4 shows the values of the estimated kinetic constants for both routes. One can notice that
334 the standard deviation values are very low for the non-catalyzed route but higher for the
335 catalyzed ones. This difference can be explained by the fact that the reaction mechanism might
336 be more complex that the one derived. Nevertheless, these standard error values are acceptable.

337 As expected, activation energy for the catalyzed route is lower than for the non-catalyzed one.
338 One should keep in mind that the rate constant for the catalyzed routes was lumped with an
339 equilibrium constant.

340 A direct comparison with the other kinetic model, displayed in Table 5, cannot be done
341 because the expression of reaction rate was not the same. Zogg et al. [25] proposed a first order
342 reaction rate with respect to acetic anhydride and did not take into account the autocatalytic

effect, neither the catalytic effect of hydrochloric acid. The kinetic constants for the non-catalytic phenomenon estimated in this work can be compared with the ones obtained from References [20], [22] and [23] by keeping in mind that in these references the autocatalytic effect was not taken into account.

The activation energy, $Ea_{Hydrolysis-non.cat}$, was found to be in the same range than References [20] and [22] but lower than the one estimated in Reference [25]. The rate constants at 40°C was calculated to be: k(40°C)= $2.23 \cdot 10^{-4}$ L mol^{-1} s^{-1} for [20], k(40°C)= $2.85 \cdot 10^{-5}$ L mol^{-1} s^{-1} for [23] and k(40°C)= $6.60 \cdot 10^{-5}$ L mol^{-1} s^{-1} for [22]. Hence, the kinetic constants for the non-catalytic effect estimated in this work are closer to the ones estimated by Susanne et al. [22].

Table 4

Estimated kinetic constants **with T_{ref}=313.15K.**

Kinetic constants	**Units**	**Estimated Parameters**	**Standard Error %**
$k'_{Hydrolysis-cat}(T_{ref})$	L mol^{-1} s^{-1}	$0.983 \cdot 10^{-1}$	17.9
$Ea_{Hydrolysis-cat}$	J mol^{-1}	29700	25.4
$k_{Hydrolysis-non.cat}(T_{ref})$	L mol^{-1} s^{-1}	$0.250 \cdot 10^{-04}$	4.6
$Ea_{Hydrolysis-non.cat}$	J mol^{-1}	46000	4.3

Table 5

Kinetic constants reported in the literature.

Reference	Added catalyst	Reaction rate	k(s^{-1}) at 40°C	Ea (kJ mol^{-1})
Zogg et al. [25]	HCl	$k(T) \times [Acetic\ anhydride]$	$8.20 \cdot 10^{-03}$	56
			A (L mol^{-1} s^{-1})	**Ea(kJmol^{-1})**
Asprey et al. [20]	None	$A \times e^{\frac{-Ea}{R.T}} \times ([Acetic\ anhydride] \times [H_2O])$	2121.75	41.84
Hirota et al. [23]	None	$A \times e^{\frac{-Ea}{R.T}} \times ([Acetic\ anhydride] \times [H_2O])$	19842433.99	71
Susanne et al. [22]	None	$A \times e^{\frac{-Ea}{R.T}} \times ([Acetic\ anhydride] \times [H_2O])$	3133.79	46.02

Another interesting comparison is between the kinetics of water and acetic anhydride, methanol and acetic anhydride. Wei et al. [37] developed a kinetic model for the esterification of acetic anhydride and methanol by taking into account the side reactions of acetic acid esterification by methanol and acetic anhydride hydrolysis. They found that the activation energy for the reaction between acetic anhydride and methanol is 88.07 kJ mol^{-1}, which is higher than the one between water and acetic anhydride. Hence, the nucleophilic attack by water is faster than by methanol.

372

373

374 3.7. Validation of the model with RC1

375 Similar experiments were performed in RC1 in order to compare the estimated constant in an
376 established calorimeter. The use of RC1 calorimeter system allows to have the evolution of
377 q_{loss}, Cp_R and UA with time.

378 The coefficient of determination was found to be 93.44%, which is slightly lower than the
379 previous one.

380 Table 6 shows that the estimated kinetics are similar than the one obtained in handmade
381 reactor, showing the reliability of this latter system.

382 **Table 6**
383 Estimated kinetic constants with RC1 and T_{ref}=313.15K.
384

Kinetic constants	**Units**	**Estimated parameter**	**Standard error %**
$k'_{Hydrolysis-cat}(T_{ref})$	L mol^{-1} s^{-1}	0.105	29.2
$Ea_{Hydrolysis-cat}$	J mol^{-1}	29600	45.3
$k_{Hydrolysis-non.cat}(T_{ref})$	L mol^{-1} s^{-1}	$0.279 \cdot 10^{-04}$	5.0
$Ea_{Hydrolysis-non.cat}$	J mol^{-1}	42100	11.0

385

386 Fig. 10 shows the fitting of experimental temperature by the simulation for Run 7.

387

388

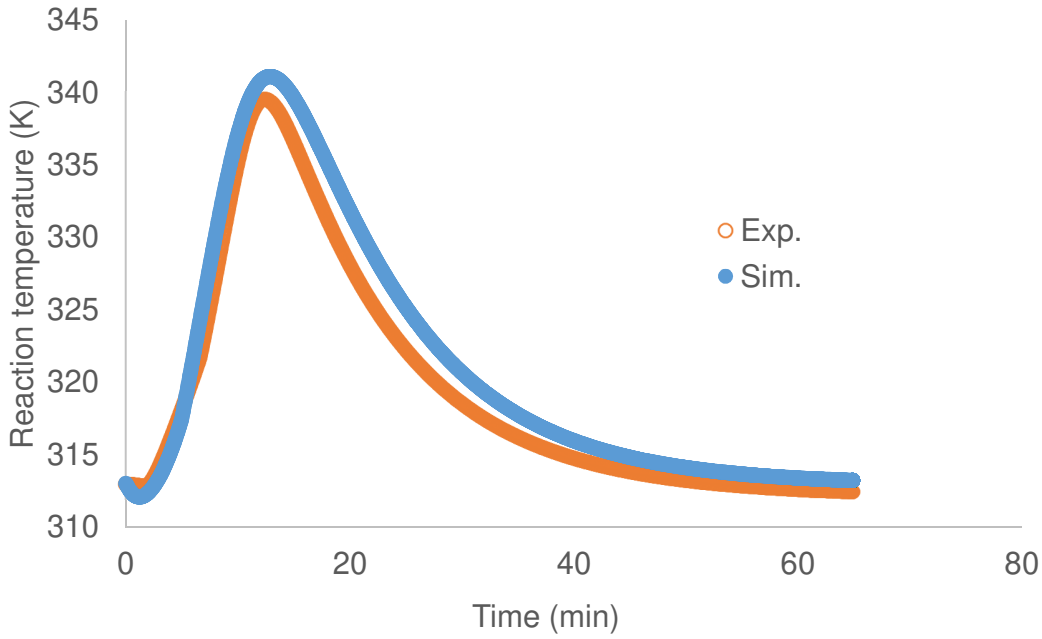


Fig. 10. Fitting of the model to the experimental data for Run 7.

4. CONCLUSIONS

This study proposes a revisited kinetic study of the hydrolysis of acetic anhydride by using temperature as an online signal.

A hand-made calorimeter was thermally characterized to be able to evaluate the heat transfer coefficient, specific heat capacity of the inserts and heat loss. Kinetic experiments were performed under isoperibolic and semibatch mode. To develop a kinetic model, the following parameters were varied: time of addition, initial reaction temperature and amount of acetic anhydride added into the reactor.

The kinetic model, using the handmade calorimeter, was developed by taking into account two routes: non-catalyzed and the catalyzed reaction due to the dissociation of the product acetic acid. The following thermal phenomena were also included: reaction enthalpy, mixing enthalpies and heat loss. It was found that the activation energy of the catalyzed route is lower than the non-catalyzed one.

To validate the results found in handmade calorimeter, experiments were performed in RC1. The estimated kinetic constants in RC1 were similar to the one in the handmade calorimeter.

NOMENCLATURE

$\bar{C}_P$	Capacity per mol, J mol^{-1} K^{-1}
[i]	Concentration of compound *i*
$\hat{C}_P$	Capacity per mass, J g^{-1} K^{-1}
d	Diameter, m
Ea	Activation energy, J mol^{-1}
k	Rate constant, L mol^{-1} s^{-1}
K	Equilibrium constant
K^C	Dissociation constant
K^T	Thermodynamic constant
m	Mass, kg
N	Rotating speed, rps
Q	Volumetric flow rate, L s^{-1}
q_{acc}	Accumulated heat-flow rate, J s^{-1}
q_{dosing}	Heat-flow rate due to dosing, J s^{-1}
$q_{exchange\ with\ heat\ carrier}$	Heat-flow rate exchange with heat carrier, J s^{-1}
q_{loss}	Heat-flow rate lossed, J s^{-1}

$q_{reaction}$	Heat-flow rate due to chemical reaction, J s^{-1}
$q_{solvation}$	Heat-flow rate of solvation, J s^{-1}
R_i	Reaction rate, mol L^{-1} s^{-1}
t	Time, s
T	Temperature, K
UA	Overall heat-transfer coefficient, W K^{-1}
V	Volume, L
ΔH	Enthalpy, J mol^{-1}
$1/h$	Convective resistance, K m^{-2} W^{-1}

Greek letters

μ	Dynamic viscosity, kg m^{-1} s^{-1}
λ	Thermal conductivity, W m^{-1} K^{-1}
ω	Mass fraction
ρ	Density, kg m^{-3}

Subscripts

0	Time zero
ambient	Ambient
Cat.	catalyzed reaction
feed	Feed
Hydrolysis-cat.	catalyzed hydrolysis reaction
Hydrolysis-non.cat	non-catalyzed hydrolysis reaction
i	Component *i*
ins	inserts
j	Jacket
R	Reaction system
s	Stirrer
w	Wall
Ref.	Reference

ACKNOWLEDGEMENTS

This study has been done in the framework of Task 2: “Green process: 2nd generation of biomass” of AMED project. The authors thank AMED project. The AMED project has been funded with the support from the European Union with the European Regional Development Fund (ERDF) and from the Regional Council of Normandie. The authors express their gratitude to Prof. Johan Wärnå for his help in the modeling stage. The authors thank the Ministry of High Education, Science and Technology of Dominican Republic. The authors thank the “Programme Excellence Eiffel”.

REFERENCES

[1] X. Cai, K. Ait Aissa, L. Estel, S. Leveneur, Investigation of the Physicochemical Properties for Vegetable Oils and Their Epoxidized and Carbonated Derivatives, J. Chem. Eng. Data. 63 (2018) 1524–1533. doi:10.1021/acs.jced.7b01075.

[2] Q. Xu, J. Ding, S. Yang, S. Ye, Measurement and calculation method of changing heat capacities during the reaction, Thermochim. Acta. 675 (2019) 55–62. doi:10.1016/j.tca.2019.03.004.

[3] E. Hanitzsch, Messung der spezifischen wärmekapazität - vergleich zwischen DSC- und pulsmethode, Thermochim. Acta. 151 (1989) 289–293. doi:10.1016/0040-6031(89)85357-2.

[4] S.Q. Miao, H.P. Li, G. Chen, Temperature dependence of thermal diffusivity, specific heat capacity, and thermal conductivity for several types of rocks, J. Therm. Anal. Calorim. 115 (2014) 1057–1063. doi:10.1007/s10973-013-3427-2.

[5] W.Y. Pérez-Sena, X. Cai, N. Kebir, L. Vernières-Hassimi, C. Serra, T. Salmi, S. Leveneur, Aminolysis of cyclic-carbonate vegetable oils as a non-isocyanate route for the synthesis of polyurethane: A kinetic and thermal study, Chem. Eng. J. 346 (2018) 271–280. doi:10.1016/j.cej.2018.04.028.

[6] I. Bylina, L. Trevani, S.C. Mojumdar, P. Tremaine, V.G. Papangelakis, Measurement of reaction enthalpy during pressure oxidation of sulphide minerals, J. Therm. Anal. Calorim. 96 (2009) 117–124. doi:10.1007/s10973-008-9883-4.

[7] R. André, M. Giordano, C. Mathonat, R. Naumann, A new reaction calorimeter and calorimetric tools for safety testing at laboratory scale, Thermochim. Acta. 405 (2003) 43–50. doi:10.1016/S0040-6031(03)00129-1.

[8] S. Leveneur, M. Pinchard, A. Rimbault, M. Safdari Shadloo, T. Meyer, Parameters affecting thermal risk through a kinetic model under adiabatic condition: Application to liquid-liquid reaction system, Thermochim. Acta. 666 (2018) 10–17. doi:10.1016/j.tca.2018.05.024.

[9] K.-Y. Chen, S.-H. Wu, Y.-W. Wang, C.-M. Shu, Runaway reaction and thermal hazards simulation of cumene hydroperoxide by DSC, J. Loss Prev. Process Ind. 21 (2008) 101–109. doi:10.1016/j.jlp.2007.09.002.

[10] A. Keller, D. Stark, H. Fierz, E. Heinzle, K. Hungerbühler, Estimation of the time to maximum rate using dynamic DSC experiments, J. Loss Prev. Process Ind. 10 (1997) 31–41. doi:10.1016/S0950-4230(96)00037-X.

[11] O.R. Valdes, V.C. Moreno, S. Waldram, L. Véchot, M.S. Mannan, Runaway decomposition of dicumyl peroxide by open cell adiabatic testing at different initial conditions, Process Saf. Environ. Prot. 102 (2016) 251–262. doi:10.1016/j.psep.2016.03.021.

[12] Y. Wang, L. Vernières-Hassimi, V. Casson-Moreno, J.-P. Hébert, S. Leveneur, Thermal Risk Assessment of Levulinic Acid Hydrogenation to γ-Valerolactone, Org. Process Res. Dev. 22 (2018) 1092–1100. doi:10.1021/acs.oprd.8b00122.

[13] A. Zogg, F. Stoessel, U. Fischer, K. Hungerbühler, Isothermal reaction calorimetry as a tool for kinetic analysis, Thermochim. Acta. 419 (2004) 1–17. doi:10.1016/j.tca.2004.01.015.

[14] L. Vernières-Hassimi, A. Dakkoune, L. Abdelouahed, L. Estel, S. Leveneur, Zero-Order Versus Intrinsic Kinetics for the Determination of the Time to Maximum Rate under Adiabatic Conditions (TMRad): Application to the Decomposition of Hydrogen Peroxide, Ind. Eng. Chem. Res. 56 (2017) 13040–13049. doi:10.1021/acs.iecr.7b01291.

[15] E. Marco, S. Cuartielles, J.A. Peña, J. Santamaria, Simulation of the decomposition of di-cumyl peroxide in an ARSST unit, Thermochim. Acta. 362 (2000) 49–58. doi:10.1016/S0040-6031(00)00587-6.

[16] I. Dobrosavljevic, E. Schaer, J.M. Commenge, L. Falk, Intensification of a highly exothermic chlorination reaction using a combined experimental and simulation approach for fast operating conditions prediction, Chem. Eng. Process. Process Intensif. 105 (2016) 46–63. doi:10.1016/j.cep.2016.04.007.

[17] M.J. Todd, J. Gomez, Enzyme kinetics determined using calorimetry: a general assay for enzyme activity?, Anal. Biochem. 296 (2001) 179–187. doi:10.1006/abio.2001.5218.

[18] W. Hoffmann, Y. Kang, J.C. Mitchell, M.J. Snowden, Kinetic Data by Nonisothermal Reaction Calorimetry: A Model-Assisted Calorimetric Evaluation, Org. Process Res. Dev. 11 (2007) 25–29. doi:10.1021/op060144j.

[19] T.J. Snee, C. Bassani, J.A.M. Ligthart, Determination of the thermokinetic parameters of an exothermic reaction using isothermal, adiabatic and temperature-programmed calorimetry in conjunction with spectrophotometry, J. Loss Prev. Process Ind. 6 (1993) 87–94. doi:10.1016/0950-4230(93)90005-I.

[20] S.P. Asprey, B.W. Wojciechowski, N.M. Rice, A. Dorcas, Applications of temperature scanning in kinetic investigations: The hydrolysis of acetic anhydride, Chem. Eng. Sci. 51 (1996) 4681–4692. doi:10.1016/0009-2509(96)00306-5.

[21] F.L. Wiseman, New insight on an old reaction – the aqueous hydrolysis of acetic anhydride, J. Phys. Org. Chem. 25 (2012) 1105–1111. doi:10.1002/poc.2945.

[22] F. Susanne, D.S. Smith, A. Codina, Kinetic Understanding Using NMR Reaction Profiling, Org. Process Res. Dev. 16 (2012) 61–64. doi:10.1021/op200202k.

[23] W.H. Hirota, R.B. Rodrigues, C. Sayer, R. Giudici, Hydrolysis of acetic anhydride: Non-adiabatic calorimetric determination of kinetics and heat exchange, Chem. Eng. Sci. 65 (2010) 3849–3858. doi:10.1016/j.ces.2010.03.028.

[24] A. Zogg, U. Fischer, K. Hungerbühler, A New Small-Scale Reaction Calorimeter That Combines the Principles of Power Compensation and Heat Balance, Ind. Eng. Chem. Res. 42 (2003) 767–776. doi:10.1021/ie0201258.

[25] A. Zogg, U. Fischer, K. Hungerbühler, A new approach for a combined evaluation of calorimetric and online infrared data to identify kinetic and thermodynamic parameters of a chemical reaction, Chemom. Intell. Lab. Syst. 71 (2004) 165–176. doi:10.1016/j.chemolab.2004.01.025.

[26] M.Á. Gómez García, I. Dobrosz-Gómez, J.C. Ojeda Toro, Thermal stability and dynamic analysis of the acetic anhydride hydrolysis reaction, Chem. Eng. Sci. 142 (2016) 269–276. doi:10.1016/j.ces.2015.12.003.

506 [27] N. Asiedu, D. Hildebrandt, D. Glasser, Kinetic Modeling of the Hydrolysis of Acetic
507 Anhydride at Higher Temperatures using Adiabatic Batch Reactor (Thermos-Flask), in: 2013.
508 doi:10.4172/2157-7048.1000176.

509 [28] J.L. Zheng, J. Wärnå, T. Salmi, F. Burel, B. Taouk, S. Leveneur, Kinetic modeling
510 strategy for an exothermic multiphase reactor system: Application to vegetable oils epoxidation
511 using Prileschajew method, AIChE J. 62 (2016) 726–741. doi:10.1002/aic.15037.

512 [29] S. Leveneur, M. Thönes, J.-P. Hébert, B. Taouk, T. Salmi, From Kinetic Study to
513 Thermal Safety Assessment: Application to Peroxyformic Acid Synthesis, Ind. Eng. Chem.
514 Res. 51 (2012) 13999–14007. doi:10.1021/ie3017847.

515 [30] I. Dobrosavljevic, E. Schaer, J.M. Commenge, L. Falk, Intensification of a highly
516 exothermic chlorination reaction using a combined experimental and simulation approach for
517 fast operating conditions prediction, Chem. Eng. Process. Process Intensif. 105 (2016) 46–63.
518 doi:10.1016/j.cep.2016.04.007.

519 [31] K. Sue, F. Ouchi, K. Minami, K. Arai, Determination of Carboxylic Acid Dissociation
520 Constants to 350 °C at 23 MPa by Potentiometric pH Measurements, J. Chem. Eng. Data. 49
521 (2004) 1359–1363. doi:10.1021/je049923q.

522 [32] S. Leveneur, L. Vernieres-Hassimi, T. Salmi, Mass & energy balances coupling in
523 chemical reactors for a better understanding of thermal safety, Educ. Chem. Eng. 16 (2016)
524 17–28. doi:10.1016/j.ece.2016.06.002.

525 [33] http://www.stenutz.eu/chem/solv6.php?name=acetic%20anhydride, acetic anhydride,
526 (n.d.). http://www.stenutz.eu/chem/solv6.php?name=acetic%20anhydride (accessed June 29,
527 2019).

528 [34] F. Lavanchy, Development of reaction calorimetry applied to supercritical CO2 and
529 methanol-CO_2 critical mixture, Infoscience. (2005). doi:10.5075/epfl-thesis-3228.

530 [35] H. Rakotondramaro, J. Wärnå, L. Estel, T. Salmi, S. Leveneur, Cooling and stirring
531 failure for semi-batch reactor: Application to exothermic reactions in multiphase reactor, J.
532 Loss Prev. Process Ind. 43 (2016) 147–157. doi:10.1016/j.jlp.2016.05.011.

533 [36] H. Haario, MODEST-User's Guide, (2001).

534 [37] H.-Y. Wei, Z.-C. Guo, L. Hao, W.-S. Bai, R. Wang, S. Li, identification of the kinetic
535 parameters and autocatalytic behavior in esterification via isoperibolic reaction calorimetry,
536 Org. Process Res. Dev. 20 (2016) 1416-1423. doi: 10.1021/acs.oprd.5b00395
537

538
539
540